

Shear Strength Assessment of Moist Sands Using Direct Shear Tests

Riju Chandra Saha

Memorial University of Newfoundland

Ashutosh Sutra Dhar (✉ asdhar@mun.ca)

Memorial University of Newfoundland <https://orcid.org/0000-0001-5137-3921>

Research Article

Keywords: Manufactured Sand, Moist Sand, Direct Shear Test, Shear Strength, Friction Angle

Posted Date: February 15th, 2022

DOI: <https://doi.org/10.21203/rs.3.rs-334904/v1>

License:   This work is licensed under a Creative Commons Attribution 4.0 International License.

[Read Full License](#)

Abstract

Granular materials are commonly used to backfill buried structures due to its free-draining property and higher shearing resistance. Conventional analysis of soil-structure interaction is performed assuming soil parameters based on typical values available in published literature for the standard and natural soils. Engineers often require replacing natural sand with locally manufactured sand as a backfill material for buried structures due to the scarcity of material and environmental considerations. This thesis presents a laboratory investigation of a locally manufactured sand which is classified as well-graded clean sand. Considering the various factors on which the strength parameters of soil depend, a series of direct shear tests are performed with varying density, normal stress, moisture content, shear displacement rate. As the soil used as a backfill for the buried structure is usually moist (unsaturated), the entire test program focuses on investigating the behavior of moist sand. The conventional test apparatus is used in this study as the special apparatus typical used in the research with unsaturated soil is not readily available to the practicing engineer. The study reveals that the conventional test apparatus can reasonably be used to estimate the design parameters for moist sand. For the manufactured sand used in this study, the effect of capillary suction on the shear strength parameters is found to be less significant. While the strength parameters depend on the degree of saturation, these depend extensively on the dry density of the soil with a higher angle of internal friction for the soil with higher dry density.

1. Introduction

The granular material is considered the most suitable backfill material for buried structures (Zornberg and Mitchell 1994). As the granular materials are free-draining, pore water pressure cannot build up within the soil and around the structures. However, natural sources of granular materials are dwindling worldwide due to extensive construction activities using these materials. Besides, suitable granular materials are sometimes not available near the construction sites, requiring importing materials from different areas. Importing materials can increase construction costs significantly. To limit the construction cost, coarse-grained materials manufactured through mechanically crushing rocks are being used in various construction works. However, the behaviors of the manufactured granular materials are often not well-known. Researchers employed different types of laboratory tests such as direct shear tests, triaxial tests, simple shear tests, etc., for determining soil parameters specific to the problems. Most of the test results available in the literature are for standard sands, such as silica sand, Fraser River Sand, Chiba sand, Cornell sand, RMS graded sand, and others (Robert 2017; Weerasekara 2011). The data on the behavior of sands manufactured through crushing of rocks is very limited. In this paper, an investigation of the shear strength of locally manufactured sand is presented. Since the sand around structures buried at shallow depth is not perfectly dry or saturated in the natural condition, the behavior of the sand under moist conditions is investigated.

The shear strength of the soil is conventionally assessed using the Mohr-Coulomb model, assuming the soil as saturated or dry (for coarse-grained soil) condition. The model parameters obtained from testing of saturated or dry soil may not be applicable to unsaturated soil. For example, Jung et al. (2016) and Al-

Khazaali and Vanapalli (2019) revealed that the axial pullout force of pipe in unsaturated sand could be higher than that in saturated sand. Large-scale experiments on soil-pipeline interaction conducted with Cornell sand and Tokyo gas sand suggest that the soil moisture around the pipelines should be considered as the presence of the moisture affects strength parameters of soil and soil-pipeline interaction (Robert 2010). It is, however, challenging to conduct tests and interpret test results for unsaturated soils. Researchers employed a modification of conventional direct shear or triaxial test apparatus to control matric suction during testing of unsaturated soils. This approach is usually complicated and time-consuming yet not flawless (Bai and Liu 2012; Al-Khazaali and Vanapalli 2019). Although the matric suction is applied and maintained during the tests using the apparatus, the actual matric suction in the field is usually unknown. Besides, the specialized equipment used in the research for unsaturated soil is usually not available in the geotechnical engineering laboratories commonly used in engineering practice., An indirect approach can be used without modifying the test equipment to avoid the difficulties (Fredlund et al. 1996; Vanapalli et al. 1996; Khalili and Khabbaz 1998). In the indirect approach, suction-related information is separately obtained from the Soil Water Characteristic Curve (SWCC), which can be developed using different methods (e.g., the Filter paper method). Then, the shear strength of unsaturated soil with respect to suction is predicted from the extension of the total stress approach accumulating the SWCC data, saturated soil property, and conventional shear strength test data (Fredlund and Rahardjo 1993). The indirect approach is employed in the current study using the conventional direct shear test apparatus.

The direct shear test is the most commonly used test method for the determination of shear strength parameters of sand. Through a series of direct shear tests on standard Ottawa sand with variable void ratios and normal stresses, Taylor (1948) revealed that the angle of internal friction of the sand decreases with the increase in void ratio and decrease in density. At each void ratio, the angle of internal friction decreases with the increase of normal stress. The decrease of shearing resistance with the increase of normal stress is attributed to the reduction of the interparticle friction coefficient due to the breakage of particles at contacts and polishing the particle surfaces with the increase of interparticle contact forces. As a result, the shearing resistance from the interparticle sliding and rolling friction is reduced (Duncan et al. 2014; Terzaghi et al. 1996). However, the void ratio has a more dominant impact on reducing the angle of internal friction than the normal stress.

Wei et al. (2018) conducted direct shear tests on soil-rock mixtures with variable moisture content from 3% to 13%. They found that the ratio of shear stress to normal stress (i.e., shear stress ratio) decreases with the increase of the normal stress. However, the shear stress ratio decreases gradually with the increase of moisture content up to 8%. The direct shear tests were also conducted at various shear displacement rates (2, 5, 10, 20 mm/min) under four different normal stresses (100 kPa, 200 kPa, 400 kPa & 800 kPa) (Wei et al. 2018). It revealed that the stress ratio increases with the increase in the shear displacement rate. However, beyond the rate of 10 mm/min, the change in stress ratio was negligible. The direct shear test was also conducted on five gravel mixtures with maximum particle size from 20 mm to 60 mm and normal stresses from 100 to 250 kPa (Wang et al. 2013). The results showed a reduction of

stress ratio with the increase of the normal stress and an increase of angle of internal friction with mean particle size and gravel contents.

In the current study, a laboratory test program was undertaken to investigate the effects of density, normal stress, rate of loading, and water contents on the behavior of the locally manufactured sand. The test program was divided into two segments, namely Test Program 1 and Test Program 2. Test Program 1 was designed for comparison of the behavior of the local sand with standard silica sand at low-stress levels (12.5 kPa – 50 kPa). Low stresses are typically expected at a shallow depth, such as backfill around the buried structures. Tests were conducted at a constant shearing rate of 1 mm/min. The moisture content in the soil was varied up to around 3%. A total of 42 direct shear tests have been completed in this test program. Test Program 2 was designed to conduct a more elaborate study of the behavior of the sand, varying the moisture content and normal stress over a wider range. The rate of shearing was also varied to examine the effects. A total of 80 direct shear tests were completed in Test Program 2.

2. Test Material

A locally manufactured sand and silica sand were used in the overall test program. Fig. 1 shows the grain size distribution of the sands. It reveals the local sand are well-graded clean sand with the median particle size (D_{50}) of 0.742 mm, the uniformity coefficient (C_u) of 5.81, and the coefficient of curvature (C_c) of 2.04. It has a fines content of around 1.3% and gravel content of around 0.87%. The silica sand is poorly graded sand with the median particle size (D_{50}) of 0.22 mm, the uniformity coefficient (C_u) of 2.04, and the coefficient of curvature (C_c) of 1.09.

Jung et al. (2016) presented different grain-size distribution zones depending on the suction effects on the buried pipe. The zones are identified as negligible, low, moderate, and a high potential for suction effects depending on the increasing trend of lateral soil-pipe reaction force for soils with different grain size distributions. The local sand predominantly falls within the low suction effect zones, and the silica sand falls in the zone of moderate to high suction effects in the chart of Jung et al. (2016).

A Standard Proctor compaction test was conducted for each of the samples. The compaction curves are shown in Fig. 2. In Fig. 2, the dry densities are the maximum at the zero-moisture content (dry condition), which are 18.8 kN/m³ and 15.5 kN/m³ for the local sand and the silica sand, respectively. In cohesionless soil, the unit weight can be the maximum at the dry condition when the particles can roll over each other during compaction/vibration. With the addition of water, capillary actions may prohibit particle movements. The effect of capillary tension at lower moisture content dominates the lubrication effect of the water, resulting in lower dry unit weight. At higher moisture contents, the capillary action diminishes, which causes an increase in the dry unit weight. As seen in Figure 3, the dry density starts to increase at moisture content beyond 4% and 6% for the local sand and silica sand, respectively. The maximum standard Proctor dry densities (SPMDD) under wet conditions for the sands are 18.0 kN/m³ and 15.1 kN/m³, and the corresponding optimum moisture contents (OMC) are 10.4% and 15%, respectively. The

optimum moisture contents are at around the water holding capacity of the sand, beyond which the water was found to drain freely through the soil.

3. Sample Preparation

Samples for the direct shear tests are prepared with different moisture contents and compaction levels. The samples are compacted to three compaction levels: high compaction, medium compaction, and no compaction denoted as H, M, and N, respectively. To achieve the high compaction, the sample is poured into the shear box in three layers with a spoon. Each layer is compacted with 25 blows of a free-falling tamping rod from a height of 40-50 mm. The tamping rod was moved within the box to apply the same compaction energy over the whole surface. For the medium compacted soil, 4 blows were applied in each layer. After compaction, the volume and mass of the soil sample used in the shear box are measured to determine the unit weight. The sample with no compaction is prepared by filling the shear boxes with the soil spreading uniformly over the porous stone without compaction. The moist samples are prepared by placing the soil in the shear box after uniform mixing of the soil with predetermined amounts of moisture. The soil was thoroughly mixed to ensure uniformity in the moisture contents. After completion of each test, the actual moisture content of each soil sample is determined through oven-drying. Note that although the same compaction efforts were applied, the unit weights of the soil were different as the moisture contents were different.

Table 1 and Table 2 show the summaries of the test program. In Test Program 1 (Table 1), the local sand and the silica sand are considered at the dry condition and three different target moisture contents (1%, 2%, and 3%, respectively). The actual moisture contents of the sand are determined after the tests. Three levels of compaction (high, medium, and no compaction) are considered for the dry soil to investigate the effect of compactions. Two levels of compaction (high and no compaction) are considered for the moist soil and during the tests conducted in Test Program 2. The moisture contents and the average densities measured during the tests are shown in the tables. A shear displacement rate of 1 mm/min is applied in Test Program 1. The shear displacement rate is also varied from 0.25 mm/min to 1.5 mm/min in Test Program 2.

Table 1. Test program 1

Test No.	Sand Type	Moisture Content (%)	Compaction	Dry Unit Weight (kN/m ³)	Sample ID	Normal Stress (kPa)
1-3	Local sand	0	High Compaction	19.05	AH0	12.5, 25, 50
4-6			Medium Compaction	18.14	AM0	
7-9			No Compaction	16.13	AN0	
10-12		0.80	High Compaction	18.45	AH1	
13-15		1.25	No Compaction	13.50	AN1	
16-18		1.20	High Compaction	17.49	AH2	
19-21		2.0	No Compaction	12.71	AN2	
22-24		2.6	High Compaction	17.32	AH3	
25-27		2.7	No Compaction	12.47	AN3	
28-30	Silica sand	0	High Compaction	16.21	CH0	
31-33			Medium Compaction	15.41	CM0	
34-36			No Compaction	14.47	CN0	
37-39		1.5	High Compaction	14.76	CH1	
40-42		3	High Compaction	14.7	CH2	
A = Local Sand, C = Silica Sand, H = High compaction, M = Medium compaction, N = No compaction, 0 = Dry Sample, 1, 2 & 3 for three moisture contents						

Table 2. Test program 2

Test No	Soil Type	Moisture Content (%)	Compaction	Dry Unit Weight (kN/m ³)	Shearing Rate (mm/min)	Normal Stress (kPa)
1-6	Local sand	0	High compaction	18.95	1	12.5, 25, 50, 100, 200, & 400
7-12		1.5		17.39		
13-18		3		16.98		
19-24		6		17.23		
25-30		0	No compaction	16.13		
31-36		1.5		12.67		
37-42		3		11.60		
43-48		6		11.49		
49-52	0	High compaction		19.05	0.25	50, 100, 200, & 400
53-56				0.5		
57-60				1		
61-64				1.5		
65-68			No compaction	16.20	0.25	
69-72					0.5	
73-76					1	
77-80					1.5	

The soil water characteristics of the compacted local sand were determined using the filter paper method with the Whatman Grade 42 filter paper. To ensure constant density (i.e., dry unit weight) for each moisture content, a fixed amount of dry soil is mixed each time thoroughly with a desired amount of water. Half of the soil is placed and compacted inside the container up to half its height, and the filter

paper is placed on top of the layer. The remaining half of the soil is then placed and compacted to the full height of the container. The Whatman filter paper was sandwiched between two larger pore-sized filter paper to protect it from direct contact with soil particles before placing. After seven days of curing the container in an airtight Ziploc bag, the moisture content of the Whatman filter paper was measured. Based on the moisture content, the matric suction of the sample was obtained using the calibration curve in ASTM D5298-10 (2010).

Fig. 3 shows the matric suctions measured for the sand at two dry unit weights (17.0 kN/m³ and 18.5 kN/m³). The matric suctions are examined against the gravimetric moisture content and degree of saturation in the figure. The solid lines are the results for the dry density of 17.0 kN/m³, and the dotted lines are for the dry density of 18.5 kN/m³. The figure shows that the soil-water characteristics are almost the same for the two levels of density considered. The matric suction of the soil is negligible at the moisture content of around 8.5%, which corresponds to the degree of saturation of around 51%. Beyond that moisture content, free draining of water was observed, indicating that the matric suction is negligible beyond water holding capacity. The soil suction increases with the reduction of moisture content and the decrease of the degree of saturation. The maximum suctions of 93 kPa, and 95.5 kPa were observed for the soil with dry unit weights of 17 kN/m³ and 18.5 kN/m³ at the moisture contents of 1.22% and 1.04%, respectively. The corresponding degree of saturation is 6% and 7%, respectively.

The experimental data of matric suction was used to fit Van Genuchten's (1980) model (Equation 1).

$$\theta = \frac{\theta_s}{[1+(\psi/\alpha)^n]^m} \quad [1]$$

Where θ is the volumetric water content, θ_s is the saturated volumetric water content, ψ is the matric suction, and α and m are model-fitting parameters. The value of α obtained from fitting the experimental data with the model for the dry unit weights of 17 kN/m³ and 18.5 kN/m³. The volumetric water contents are calculated using the specific gravity (G_s) of the soil determined from tests (i.e., $G_s = 2.63$). The resulting parameters are shown in Table 3. A comparison of Van Genuchten's model with experimental data is shown in Fig. 4.

Table 3. SWCC fitting parameter

Dry unit weight (kN/m ³)	SWCC fitting parameters		
	α	m	n
17	0.300	0.429	1.139
18.5	0.364	0.378	1.357

4. Test Results

4.1 Test Program 1

4.1.1 Shear Strength Parameters

Fig. 5 plots the maximum shear stresses from the direct shear tests against the normal stresses. Linear regression equations with the data showed an intercept on the vertical axis, indicating a nonzero cohesion even for the dry sand. Cohesion is sometimes expected in dry sand due to interlocking between the particles (Lu and Likos 2013). However, the magnitudes of the cohesion (intercept on the vertical axis) ranges from a minimum value of 0.2 kPa for AH0 sample to a maximum value of 7.9 kPa for AH3 sample, which are practically negligible, considering the uncertainties involved in the measurements and data interpretations. Thus, the apparent cohesion for the moist soil at the water contents considered (1% to 3%) is considered negligible. The apparent cohesion in unsaturated granular material predominantly results from the capillary force due to negative pore-water pressure and surface tension (Lu et al. 2007). At very low moisture contents, air voids may be connected in the granular soil within the shear box, causing the air pressure to be the same as the atmospheric pressure. As a result, the negative pore-water pressures and the apparent cohesion can be negligible. Ravindran and Gratchev (2020) also reported a lower apparent cohesion at lower moisture content for a gravelly/sandy soil that increased initially and then decreases with the increase of water content. The slopes of the lines in Fig. 5 are different, indicating different friction angles, which is due to the combined effects of water contents and densities of the soil, as discussed later. As mentioned earlier, although the same compaction efforts were applied for the soil samples at different moisture contents, the dry densities of the soil were different.

4.1.2 Stress-Deformation Responses

Since the apparent cohesion of sand is negligible for the sand, the shear strength of the soil depends exclusively on the normal stress for each condition (i.e., stress level, density, and water content). The ratio of the shear strength to the normal stress (called herein as “stress ratio”) is therefore examined here against the shear displacements. The volumetric strain is examined in term of a dilation rate, defined as the ratio of the changes in vertical displacement change (dv) to the changes in the horizontal displacement (du) (i.e., Dilation rate), after Simoni and Houlsby (2006).

Fig. 6 shows the variation of stress ratios with horizontal displacement for four conditions of the local sand subjected to high compaction. As seen in the figure, the peak stress ratios are almost the same for all normal stresses for the dry sample (Fig. 6 (a)). However, for the moist samples, the peak stress ratio decreases with the increase of normal stress. The peak stress ratio is around 1.2 for the dry sand, which corresponds to a peak friction angle of 50° . For the moist sand, the peak stress ratio varies from 0.8 to 1.25. These correspond to friction angle variations from 38° to 51° , with the lowest value for the normal stress of 50 kPa and the highest value for the normal stress of 12.5 kPa. It is also to be noted that post-peak degradation of the stress ratio is abrupt for the dry sand, whereas the post-peak degradation is gradual for the moist sands. This may be because of capillary forces in the moist sample. For the dry

sand, the stress ratio is reduced from a peak value of 1.2 to a critical state value of around 0.7. Thus, the critical state friction angle for the soil is 35° . The critical state stress ratios for the moist samples range from 0.7 to 0.8, except for the normal stress of 12.5 kPa. For 12.5 kPa of normal stress, the stress ratios fluctuate beyond the peak values, potentially due to the low confining effects. The peak and post-peak behavior observed for the dry sand is commonly reported in the literature (Al Tarhouni et al., 2017). However, the behavior of moist sand has not been extensively investigated to examine the behaviors.

For the moist samples, the peak stress ratio is higher for soil AH1 having around 0.8% of moisture content than for AH2, having around 1.2% of moisture content at each of the stress levels considered. The shear strength is higher again for soil AH3 having a moisture content of around 2.6%. The shear strength changes are attributed to the changes in the densities of the soil prepared using the same method of compaction and the capillary actions.

Fig. 7 plots the calculated dilation rate against the horizontal displacement for the four conditions of the local sand subjected to high compaction. Each of the samples shows positive dilation rates, indicating an increase in the volume (dilation) during shearing. In general, the peak dilation rate occurs at the horizontal displacement of 1 to 2 mm. For the dry sample, the dilation rate drops rapidly after reaching the peak value. For the moist samples, the dilation rate decreases gradually with the increase in horizontal displacement, which is consistent with the changes in the stress ratios in Fig. 6. The dilation angle for each of the samples eventually reaches almost zero, which is essentially the critical state.

Fig. 8 shows the variation of stress ratio with horizontal displacement for the local sand samples prepared without compaction. For the loose condition of the soil, no post-peak degradation in the stress ratio is observed in any of the samples, as expected. As seen in Fig. 8 (b-d), the peak stress ratio is almost the same for all normal stresses for the moist samples. The peak ratios are 0.6, 0.55, and 0.5 for samples AN1, AN2, and AN3, respectively, which correspond to the friction angles of 31° , 29° and 26.5° , respectively. The moisture contents in these samples are 1.25%, 2.0%, and 2.7%, respectively. The friction angles for the loose soils are 30% to 40% less than the peak friction angles for the dense soils discussed above.

For the loose dry sand, the stress ratio appears to decrease with the increase of normal stress that varies from 0.69 to 0.88 (Fig. 8(a)). The stress ratios correspond to the friction angle of 34.5° to 41° . The higher value is for the normal stress of 12.5 kPa, and the lower value is for the normal stress of 50 kPa. Thus, the peak friction angle of the loose soil at 50 kPa is close to the critical state friction angle for the dense soil (discussed above). However, for the low normal stress of 12.5 kPa, the friction angle in the loose condition is higher than the critical state friction angle. Thus, the concept of critical state friction angle may not be applicable at the low confining pressure of the soil. Al Tarhouni et al. (2017) also questioned the critical state friction angle of sand at low confining pressure from direct simple shear and triaxial tests.

The dilation rate for the loose soil is generally negative, indicating a decrease of volume during the direct shear tests, as shown in Fig. 9. As the shearing of soil occurs at constant volume, the dilation rates

become zero at the point of shear failure. However, the increase in the volume of the soil (positive dilation rate) is observed in the dry sample during shearing (Fig. 9(a)). It shows that although the dilation rate is negative at the beginning, it increases with the increase of horizontal displacement and reaches the maximum value at the horizontal displacement of around 2 mm. The stress ratio is also peak at the same horizontal displacement (i.e., 2 mm). Similar load-deformation behavior was observed for the silica sand but has not been included here for the sake of brevity.

4.1.3 Peak Stress Ratio

As discussed earlier, the peak stress ratios obtained from different tests are found to be different. The stress ratios generally depend on the stress levels, water contents, and the densities of the soil. To examine the effect of stress levels, the peak stress ratios for various soils are plotted against normal stress in Fig. 10. The figure reveals that the stress ratio is generally the highest at the normal stress of 12.5 kPa. The changes in the stress ratios are not significant beyond the normal stress of 25 kPa. In general, the stress ratio is the highest for the dry soils and decreases with the increase in water content, except for the silica sand. Tiwari and Al-Adhath (2014) demonstrated for well-graded sand that the friction angle can decrease for changing from dry state to saturated state at the same relative density, which is likely due to the effect of lubrication around the soil particle by the water. However, the test results presented here can also depend on the density of the soil, as discussed below.

To examine the effect of water contents, the peak stress ratio at various normal stresses is plotted against the water contents in Fig. 11. Since the dry densities of the soil in the shear box are also expected to be different even under the same compaction effort, the calculated dry unit weights of the soil are also plotted against the moisture contents in this figure. It shows that the peak stress ratio and the dry unit weight of the soils decrease with the increase of moisture content. Thus, the reduction of the peak stress ratio with moisture content has a strong correlation with the reduction of the dry density. While both dry density and the water content are expected to contribute to the peak stress ratio of the soil, the contribution of each parameter could not be separated from this test program.

4.2 Test Program 2

4.2.1 Stress–Deformation Responses

Fig. 12 shows the changes in stress ratio with horizontal displacement for the compacted samples at various normal stresses. The responses are similar to those observed in Test Program 1. In Fig. 12, the changes in the peak stress ratio with the normal stress are insignificant for the dry sands (~1.2 for the normal stresses of 12.5 kPa to 100 kPa and 1.1 for the normal stresses of 200 kPa to 400 kPa). For the moist samples, the peak stress ratio is the highest for 12.5 kPa of normal stress that reduces with the increase of the normal stress. As observed in Test Program 1, the post-peak degradation of the stress ratio is rapid for the dry sand and is gradual (and less significant) for the moist sand. The dilation rates

observed in this test program were also similar to those observed in Test Program 1 (not included in this paper).

4.2.2 Peak Stress Ratio

Fig. 13 shows the variation of peak stress ratio with normal stress for the compacted and loose samples. In general, the peak stress ratio is the highest at normal stress of 12.5 kPa that decreases with the increase of the normal stress. However, the effect is less significant for the dry sand. For the dense condition of the dry sand, the changes in the peak stress ratio with the normal stress are negligible. For loose conditions of the soil, the peak stress ratio was changed from 0.93 to 0.7 for increasing the normal stress from 12.5 kPa to 400 kPa.

For the moist sand, the peak stress ratio consistently reduced with the increase of normal stress for the dense condition of the soil. However, for the loose conditions, the peak stress ratio remains almost constant (~ 0.67) for normal stresses between 100 and 400 kPa, indicating a less effect of normal stress on the peak stress ratio at high stress levels.

4.2.3 Effect of Shearing Rate

The effect of the rate of shearing on the stress ratio is studied under four normal stresses 50, 100, 200, and 400 kPa for dry sand samples only. However, no significant variation of the stress ratios with the shearing rate was observed both for dense and loose conditions of the soil. Fig. 14 shows the typical variation of stress ratio with the shearing rate observed during the tests. Lade and Nam (2009) also reported no effect of shearing on the shear strength for dry sand.

4.2.4 The Angle of Internal Friction

The above study revealed that the angle of internal friction depends on the density, stress level, and moisture content of the sand. To examine these further, the peak shear stresses from the tests are plotted against the normal stresses in Fig. 15. Test results showed that the peak shear stress versus normal stress response is almost linear at low densities of the soil (Fig. 15(a)). Beyond the density of 17 kN/m^3 , the responses are nonlinear (Fig. 15(b)). Thus, at lower densities (or unit weights) of the soil, the effect of the normal stress on the friction angle (the slope) is insignificant. However, at the higher unit weights of the soil, the friction angle is higher at lower stress levels and relatively lower at higher stress levels. In both cases, the intercepts of the shear strength versus normal stress plot are negligible even for the moist soil. Thus, the effect of suction on the shear strength (i.e., apparent cohesion) of the soil is considered negligible during the direct shear tests.

Fig. 15 reveals that the shear strength of the soil is higher for a higher density of the soils. The rate of increase of shear strength with density is relatively less for the sand with a density of less than 17 kN/m^3 . For an increase of the density from 11.5 kN/m^3 to 16.1 kN/m^3 , the shear strength increases from 256.6 kPa to 273.8 kPa at the normal stress of 400 kPa. However, for the increase of density from 17 kN/m^3 to

19 kN/m³, the shear stress increases from 290.1 kPa to 578.8 kPa at the same normal stress (i.e., 400 kPa). Thus, the effect of density on the shear strength (hence, the angle of internal friction) is very significant at the dense condition of the soil (>17 kN/m³).

Note that even at different moisture contents, the shear strengths are the same for the same levels of densities. In Fig. 15(b), the responses for the moisture contents of 1.5% (with $g_d = 17.4 \text{ kN/m}^3$) and 6% (with $g_d = 17.2 \text{ kN/m}^3$) match with each other. Similarly, the test results with dry unit weights of 18~19 kN/m³ match reasonably (less than 10% difference) with each other. Thus, the contribution of the moisture contents is apparently insignificant to the shear strength for the levels of moisture contents considered.

The angles of internal friction of the sand are calculated from the slope of linear trendlines of the peak shear stress versus normal stresses data from the tests. The calculated angles of internal friction and the dry densities are plotted against the water contents in Fig. 16. The maximum angle of internal friction of 49° is found for the compacted dry samples, which is reduced with the increase of moisture content. For the uncompacted sample, the maximum angle of internal friction is ~34.5° for the dry sand that is reduced with the moisture contents. Dry unit weights of the sand are also reduced with the increase of moisture content for both compacted and uncompacted soil. This observation confirms that the reduction of the angle of internal friction with moisture content in the tests is due to the reduction of the density (dry unit weight). Thus, the degree of compaction is the most significant controlling parameter for the shearing resistance of the soil. Note that the peak shear stress of the dry sand is close to that of the moist sand with 5.6% moisture in Fig. 15(b), as the dry unit weights of the soils are similar.

Fig. 17 plots the friction angles against the relative compaction calculated using the maximum dry density obtained from the Standard Proctor Compaction tests. As expected, the friction angle increases with the increase of the relative compaction. The rate of increase is less at lower relative compactions (loose condition), which is significantly high at high relative compactions. As seen in Fig. 17, the friction angle increases at a lower rate up to the relative compaction of 90%, a moderately high rate from 90% to 100% of relative compaction, and a very high rate beyond 100% of relative compaction. The poorly graded silica sand samples showed lower friction angles than those for the local sand at the same level of relative compactions.

5. Summary and Conclusion

The behavior of a locally manufactured sand is studied using direct shear tests under varying moisture content, compaction level, and stress level. It reveals that the cohesion resulting from matric suction is negligible for the range of moisture content considered (1% to 6%) in the direct shear test box. The sand considered here falls within the low suction effect zone according to the grain-size distribution plot in Jung et al. (2016). The soil-moisture characteristic obtained using the filter paper method reveals the soil to have negligible matric suction beyond the water content of 8.5% (degree of saturation of 51%) and 95.5 kPa of matric suction at ~1% of water content (6~7% degree of saturation). In standard Proctor

compaction tests, the sand showed the highest dry density at the zero moisture content that reduced initially with the increase of moisture content and increased again at water contents beyond 4% to 6%, reaching the maximum value at the moisture content of around 10.4%. The optimum moisture content (i.e., 10.4%) is greater than the water content beyond which the matric suction is negligible (i.e., 8.5%). Beyond this water content free draining of water was observed, indicating that as the water holding capacity of the sand. The major findings from this study are summarized below:

- The friction angle of the soil was found to depend significantly on the density of the soil, regardless of the moisture contents. In general, the friction angle was higher for dry soil that decreased with the increase of moisture content, which is due to the changes in the dry unit weight of the sand. Although a similar approach of soil compaction is used in each of the tests, the degrees of compaction of the soil samples in the test box were different due to the presence of different moisture contents. The degree of compaction is found as the dominant factor affecting the shear strength of the sand.
- The rate of increase of the friction angle with relative density is less at lower relative compactions (<90% SPMDD), moderately high between the relative compaction of 90% and 100% and very high at relative compaction greater than 100% SPMDD.
- The rate of shearing within the range of 0.25 mm/min to 1.5 mm/min was found to have an insignificant effect on the behavior of the dry sand.
- The dense sand samples showed the post-peak degradation of stress ratio. The post-peak degradation of the stress ratio is abrupt for the dry sand and gradual for the moist sands. The rate post-peak dilation also reduced rapidly in the dry sand and gradually in the moist sand. The capillary forces can influence the post-peak behavior of the moist sample.
- The peak stress ratio is generally higher at lower normal stress levels, indicating a higher friction angle for the soil at the lower confining pressure. This was particularly observed for the compacted moist samples. The changes in the peak stress ratio with the normal stress was negligible for compacted dry sand. At the loose condition, the effect of the normal stress on the friction angle was less significant.
- The peak friction angle of the loose sand matches with the critical state (constant volume) friction angle of the dense sand at high confining pressure. However, at low normal stress (i.e., 12.5 kPa), the peak friction angle of the loose soil was greater than the critical state friction angle. Thus, one should be careful in applying the concept of critical state friction angle at low confining pressure.

Declarations

Funding

The funding for this research is provided by the Collaborative Research and Development Grant program of Natural Science and Engineering Research Council of Canada, Innovate NL program of the Government of Newfoundland and Labrador, and FortisBC Energy Inc.

Conflicts of Interest/Competing Interests

No conflicts of interest.

Availability of Data and Materials

All data and materials have been included in the manuscript.

Code Availability

Not applicable

Authors' Contributions

Mr. Riju Chandra Saha conducted all tests for this research, analyzed the test results, and prepared the manuscript under the supervision of Dr. Ashutosh Sutra Dhar. Dr. Dhar planned the research program, reviewed the test plan and results, and edited the manuscript prepared by Mr. Saha.

ACKNOWLEDGMENTS

The authors gratefully acknowledge the financial and/or in-kind support for this research provided by the Collaborative Research and Development Grant program of Natural Science and Engineering Research Council of Canada, Innovate NL program of the Government of Newfoundland and Labrador, FortisBC Energy Inc. and WSP Canada Inc. The authors also appreciate the comments from Dr. Bipul Hawlader, Professor at Memorial University of Newfoundland.

References

1. Al-Khazaali M, Vanapalli SK (2019) Axial Force-Displacement Behaviour of a Buried Pipeline in Saturated and Unsaturated Sand. *Geotechnique* 69(11):986–1003.
<https://doi.org/10.1680/jgeot.17.P.116>
2. Al Tarhouni MA, Fouzder A, Hawlader B, Dhar A (2017) Direct Simple Shear and Triaxial Compression Tests on Dense Silica Sand at Low Effective Stress. In: *Proceedings of 70th Canadian Geotechnical Conference*, Ottawa, ON
3. ASTM D5298-10 (2010) Standard Test Method for Measurement of Soil Potential (Suction) Using Filter Paper. ASTM International, West Conshohocken
4. Bai FQ, Liu SH (2012) Measurement of the Shear Strength of an Expansive Soil by Combining a Filter Paper Method and Direct Shear Tests. *Geotech Test J* 35(3):451–459
5. Duncan JM, Wright SG, Brandon TL (2014) *Soil strength and slope stability*. Wiley, Hoboken
6. Fredlund DG, Rahardjo H (1993) *Soil mechanics for unsaturated soils*. Wiley, New York
7. Fredlund DG, Xing A, Fredlund MD, Barbour SL (1996) The Relationship of the Unsaturated Soil Shear Strength to the Soil-Water Characteristic Curve. *Can Geotech J* 33(3):440–448

8. Jung JK, O'Rourke TD, Argyrou C (2016) Multi-Directional Force–Displacement Response of Underground Pipe in Sand. *Can Geotech J* 53(11):1763–1781. <https://doi.org/10.1139/cgj-2016-0059>
9. Khalili N, Khabbaz MH (1998) A Unique Relationship for the Determination of the Shear Strength of Unsaturated Soils. *Geotechnique* 48(5):681–687
10. Lade PV, Nam J (2009) Strain Rate, Creep, and Stress Drop-Creep Experiments on Crushed Coral Sand. *J Geotech Geoenviron Eng* 135(7):941–954
11. Lu N, Likos WJ (2006) Suction Stress Characteristic Curve for Unsaturated Soil. *J Geotech Geoenviron Eng* 132(2):131–142
12. Lu N, Wu B, Tan CP (2007) Tensile Strength Characteristics of Unsaturated Sands. *J. Geotech. Geoenviron. Eng.* 133 (2): 144–154. [https://doi.org/10.1061/\(ASCE\)1090-0241\(2007\)133:2\(144\)](https://doi.org/10.1061/(ASCE)1090-0241(2007)133:2(144))
13. Ravindran S, Gratchev I (2020) Estimation of Shear Strength of Gravelly and Sandy Soils from Shallow Landslides. *Int J GEOMATE* 18(70):130–137
14. Robert D (2017) A Modified Mohr-Coulomb Model to Simulate the Behavior of Pipelines in Unsaturated Soils. *Comput Geotech* 91:146–160
15. Robert D (2010) Soil–Pipeline Interaction in Unsaturated Soils. Dissertation, The University of Cambridge. <https://doi.org/https://doi.org/10.17863/CAM.11686>
16. Simoni A, Houlsby GT (2006) The Direct Shear Strength and Dilatancy of Sand-Gravel Mixtures. *Geotech Geol Eng* 24(3):523–549. <https://doi.org/10.1007/s10706-004-5832-6>
17. Taylor DW (1948) *Fundamentals of Soil Mechanics*. Wiley, New York
18. Terzaghi K, Peck RB, Mesri G (1996) *Soil Mechanics in Engineering Practice*. Wiley, New York
19. Tiwari B, Al-Adhadh AR (2014) Influence of Relative Density on Static Soil-Structure Frictional Resistance of Dry and Saturated Sand. *Geotech Geol Eng* 32(2):411–427. <https://doi.org/10.1007/s10706-013-9723-6>
20. Van Genuchten MT (1980) A Closed-Form Equation for Predicting the Hydraulic Conductivity of Unsaturated Soils. *Soil Sci Soc Am J* 44:892–898
21. Vanapalli SK, Fredlund DG, Pufahl DE, Clifton AW (1996) Model for the Prediction of Shear Strength Respect to Soil Suction. *Can Geotech J* 33(3):379–392
22. Wang J, Zhang H, Tang S, Liang Y (2013) Effects of Particle Size Distribution on Shear Strength of Accumulation Soil. *J Geotech Geoenviron Eng* 139(11):1994–1997
23. Weerasekara L (2011) Pipe-Soil Interaction Aspects in Buried Extensible Pipes. Dissertation, The University of British Columbia
24. Wei HZ, Xu WJ, Wei CF, Meng QS (2018) Influence of Water Content and Shear Rate on the Mechanical Behavior of Soil-Rock Mixtures. *Sci China Technol Sci* 61(8):1127–1136
25. Zornberg JG, Mitchell JK (1994) Reinforced Soil Structures with Poorly Draining Backfills. Part I: Reinforcement Interactions and Functions. *Geosynth Int* 1(2):103–147

Figures

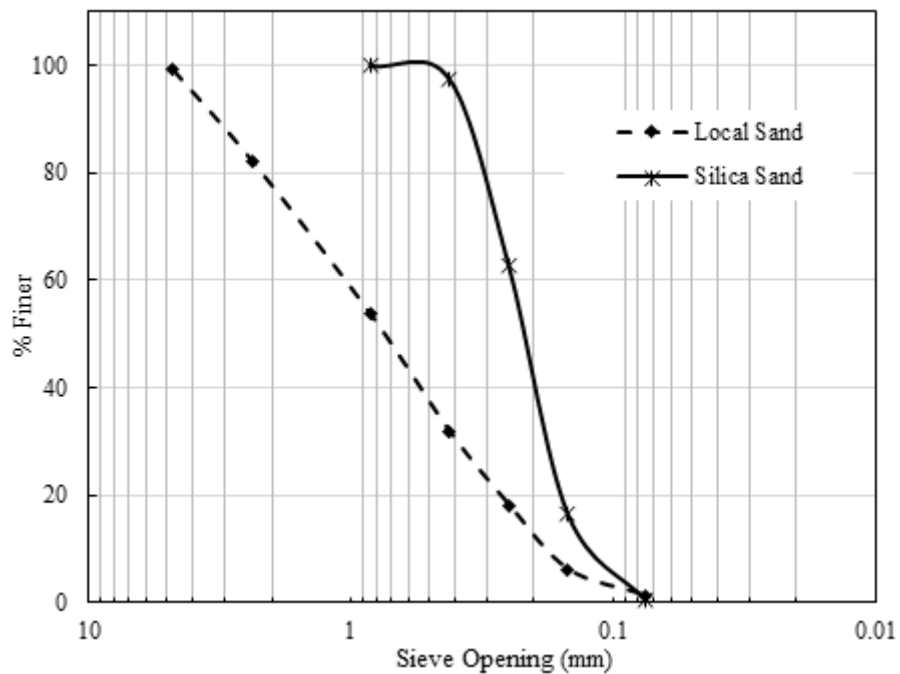


Figure 1

Grain size distribution of local sand & silica sand

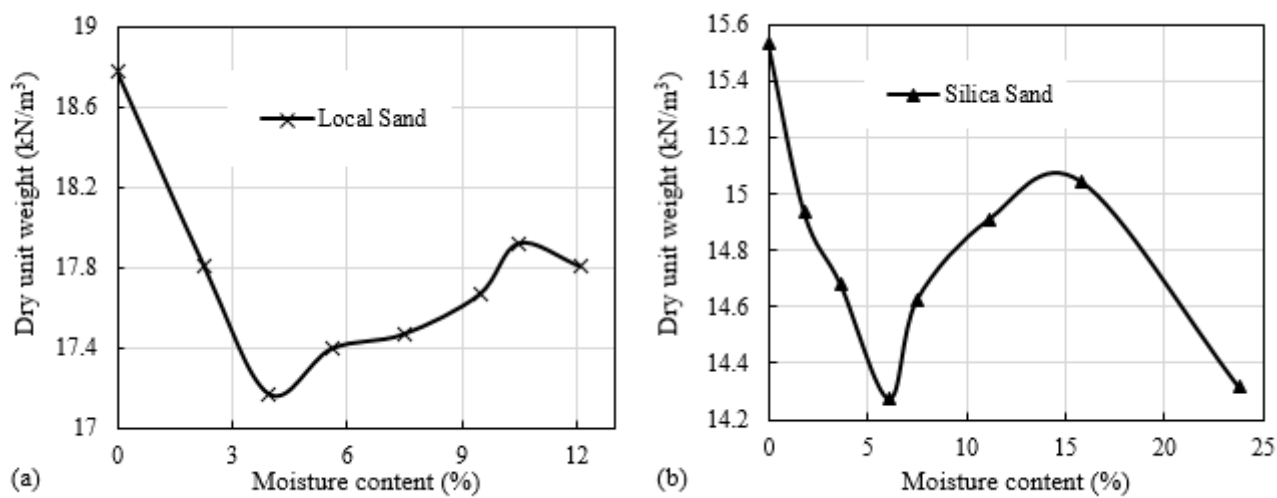


Figure 2

Results of standard proctor compaction tests: a) Local Sand, and b) Silica Sand

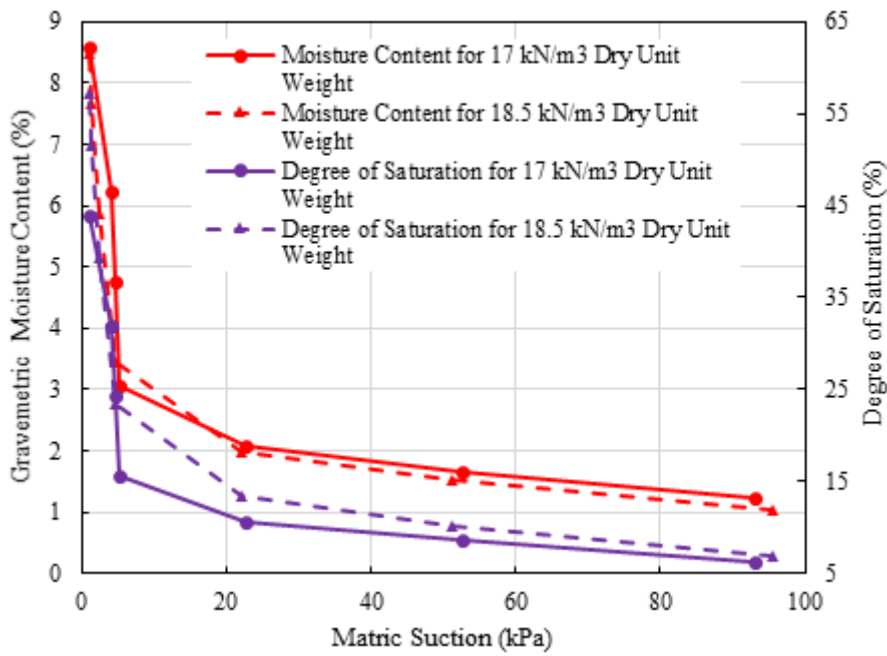


Figure 3

Soil-Water characteristic curve for sand

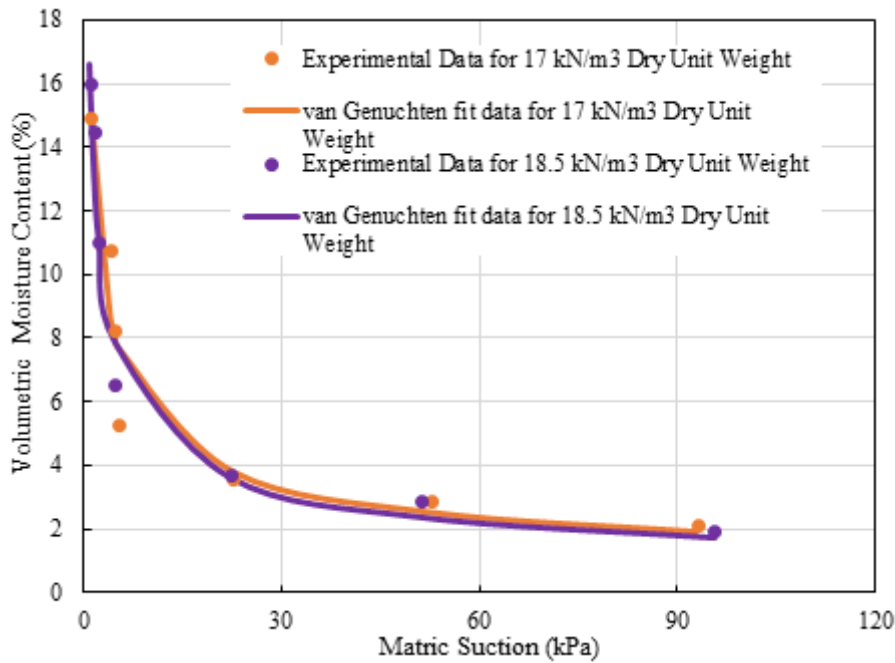


Figure 4

Comparisons of the best fit SWCC models with test data.

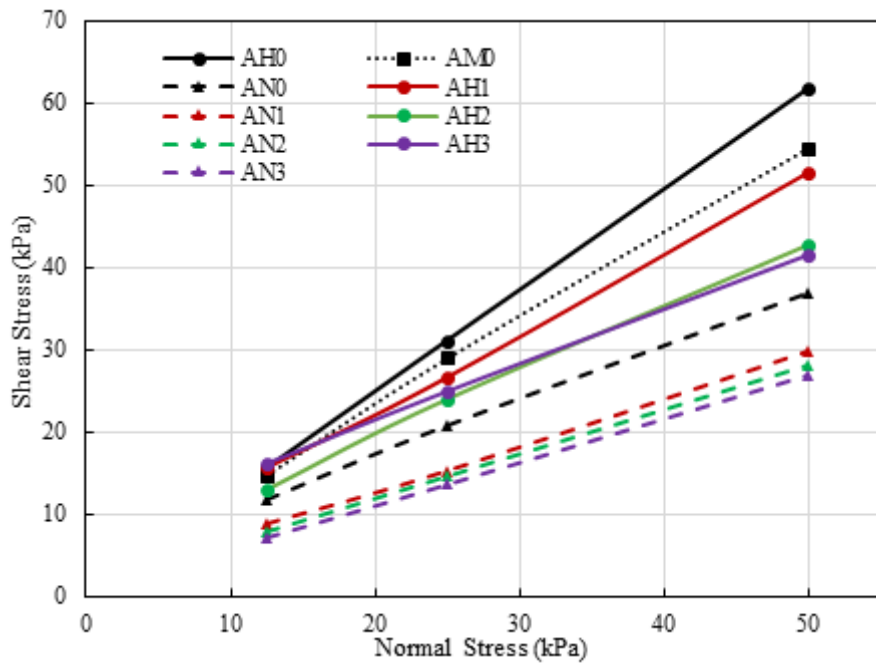


Figure 5

Shear stress-Normal stress plot for the local sand

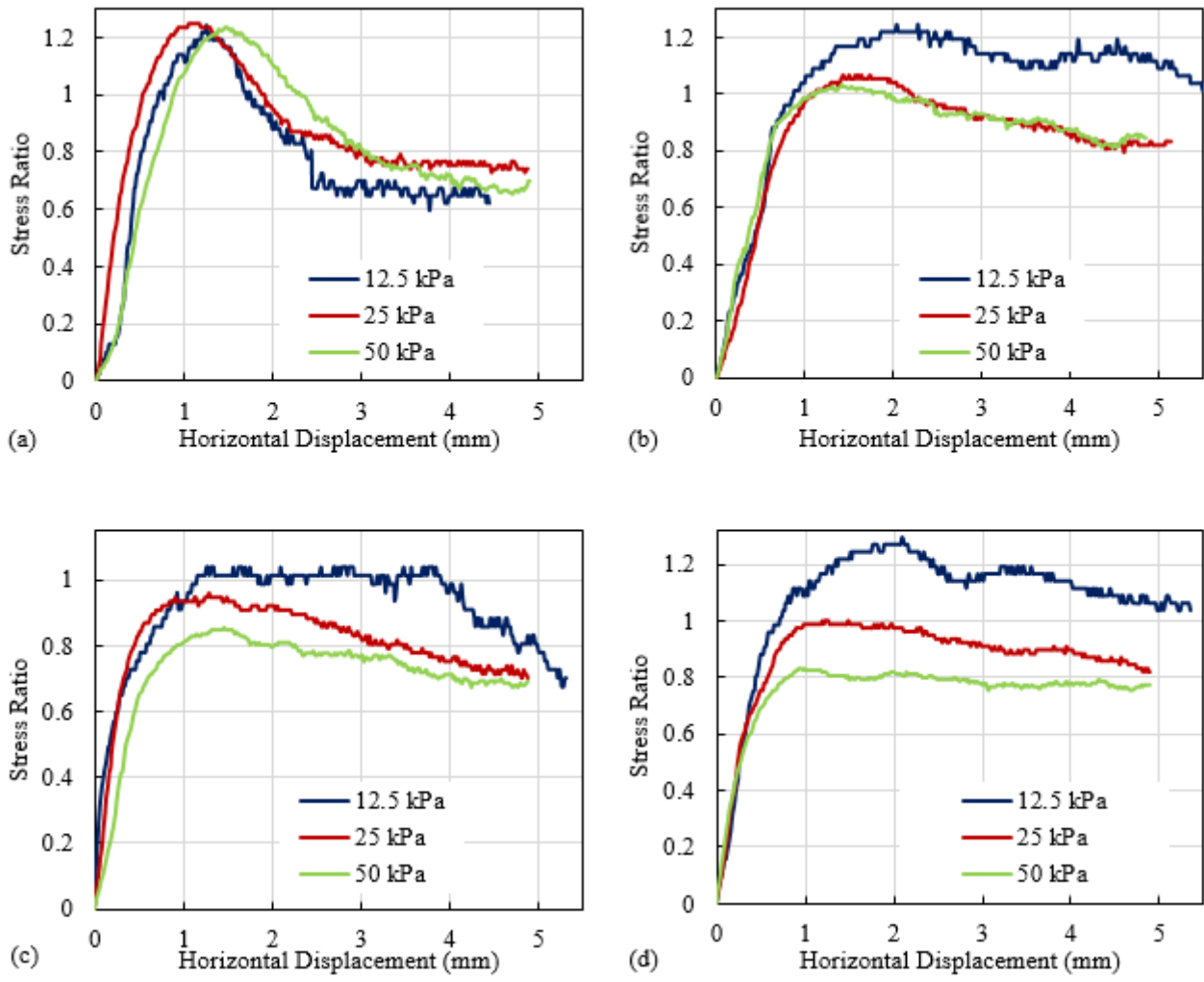


Figure 6

Variation of stress ratio for the dense condition of the local sand: a) AH0, b) AH1, c) AH2, and d) AH3

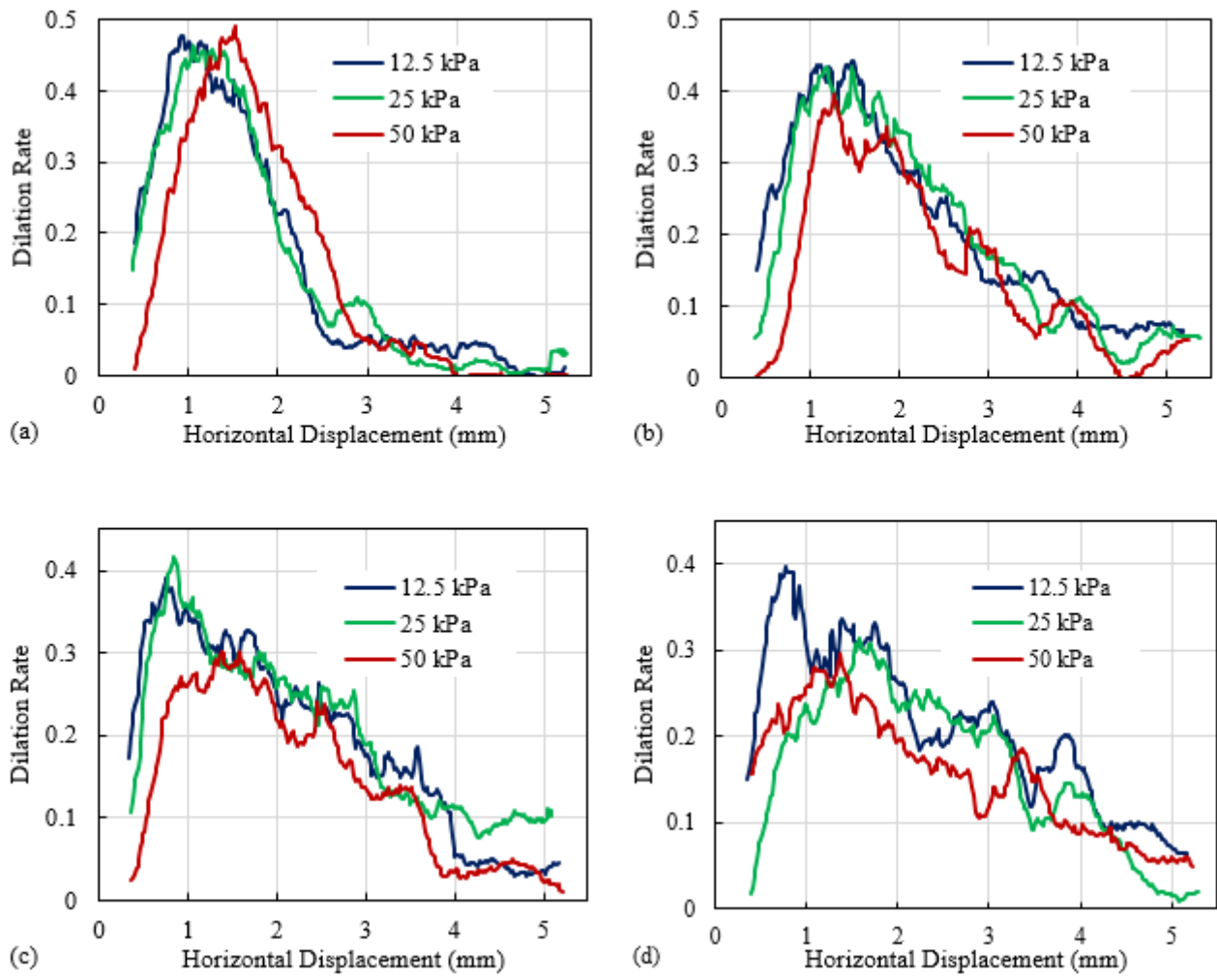


Figure 7

Dilation rates for the dense condition of sample A: a) AH0, b) AH1, c) AH2, and d) AH3

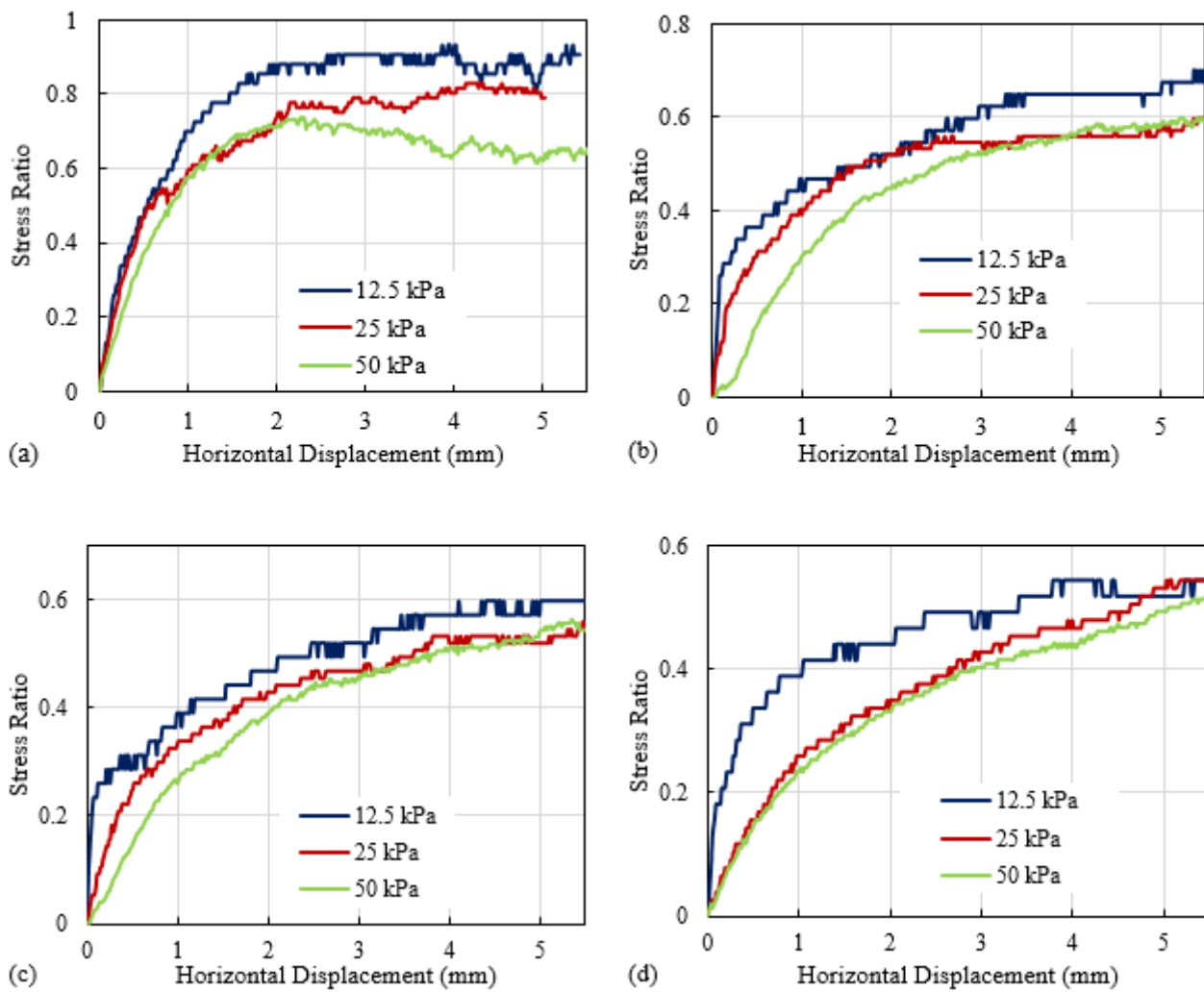


Figure 8

Variation of stress ratio for the loose condition of sample A: a) AN0, b) AN1, c) AN2, and d) AN3

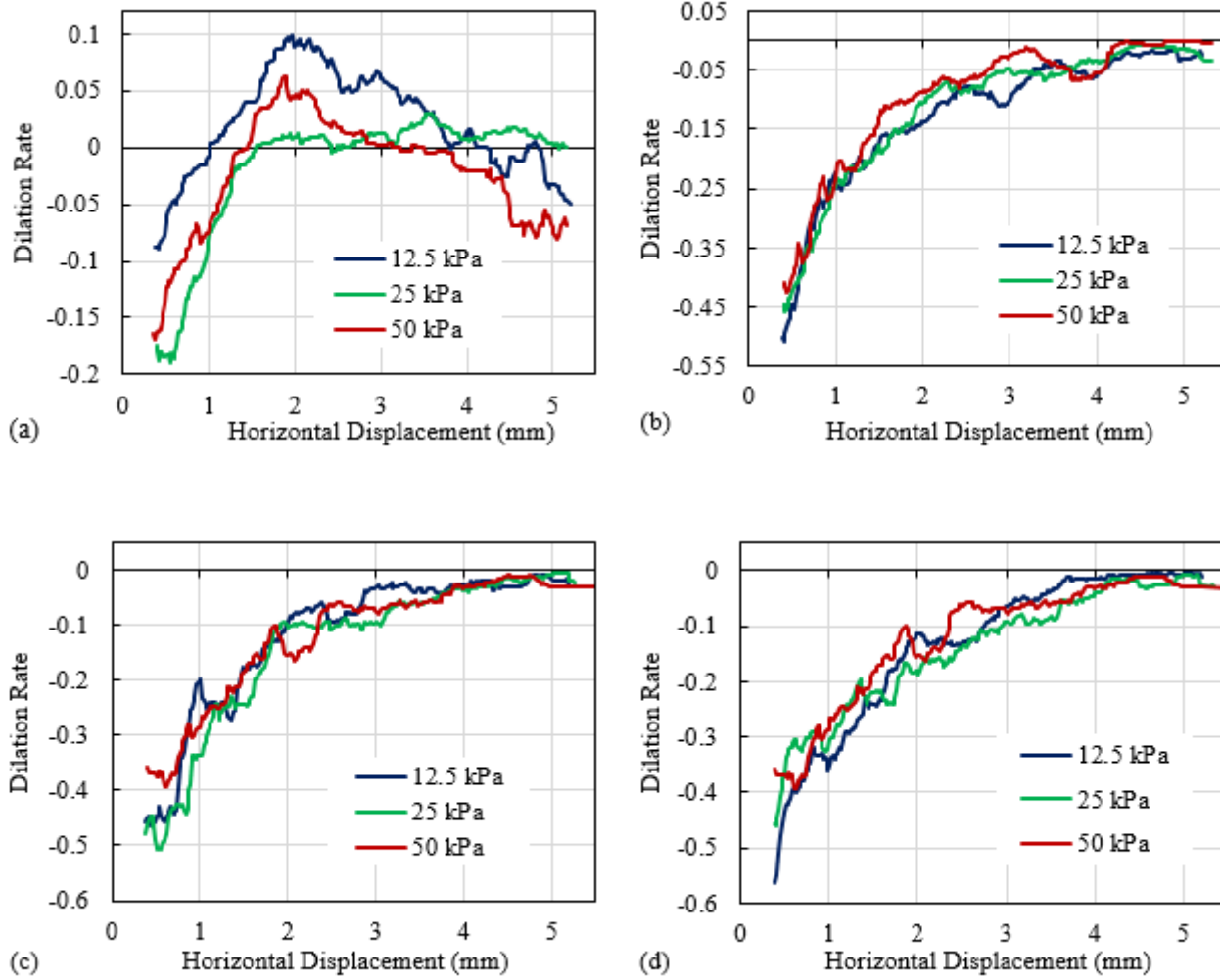


Figure 9

Dilation rates for loose condition of sample A: a) AN0, b) AN1, c) AN2, and d) AN3

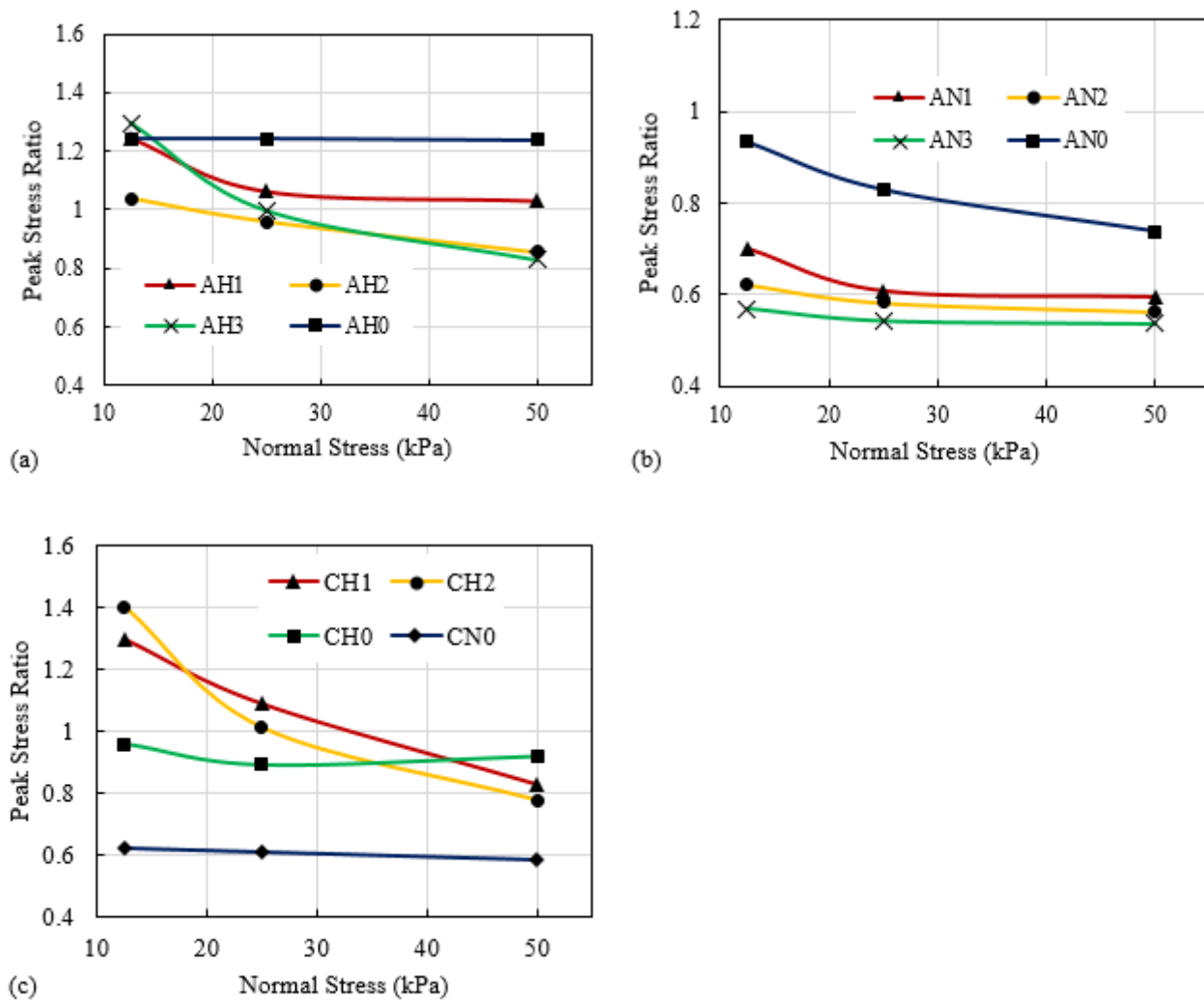


Figure 10

Effect of normal stress on peak stress ratio: a) Dense local sand, b) Loose local sand, c) Silica sand

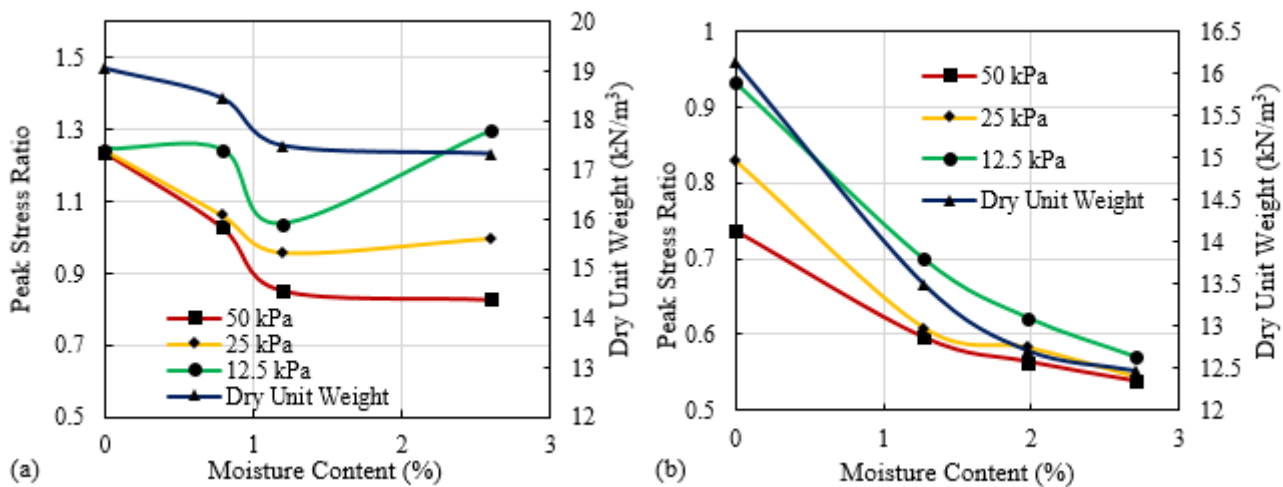


Figure 11

Effect of dry unit weight on the change of peak stress ratio with moisture content: a) Compacted local sand, b) Uncompacted local sand

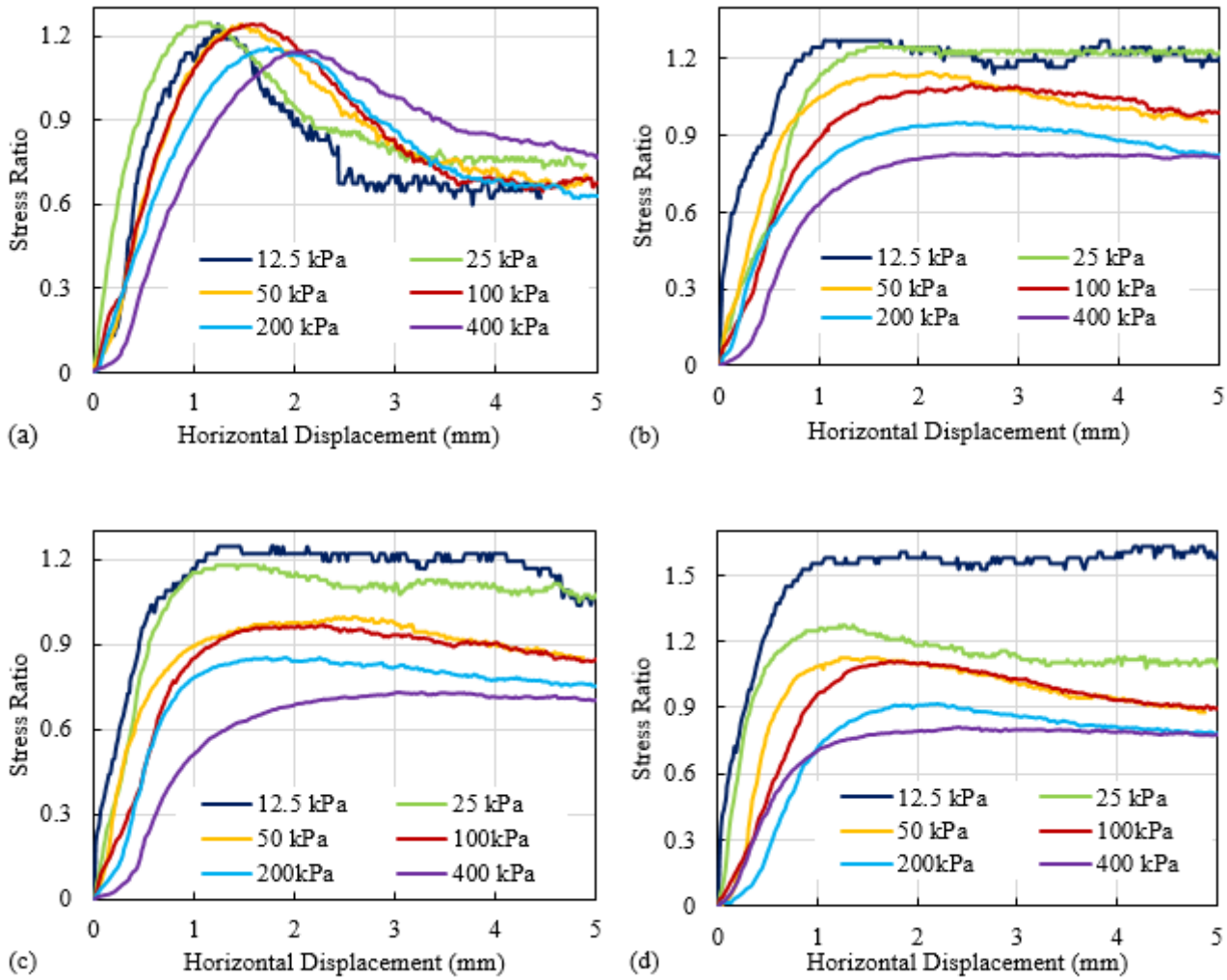


Figure 12

Stress ratio for compacted sand sample for varying moisture contents a) 0% (Dry), b) 1.5%, c) 3%, and d) 6%.

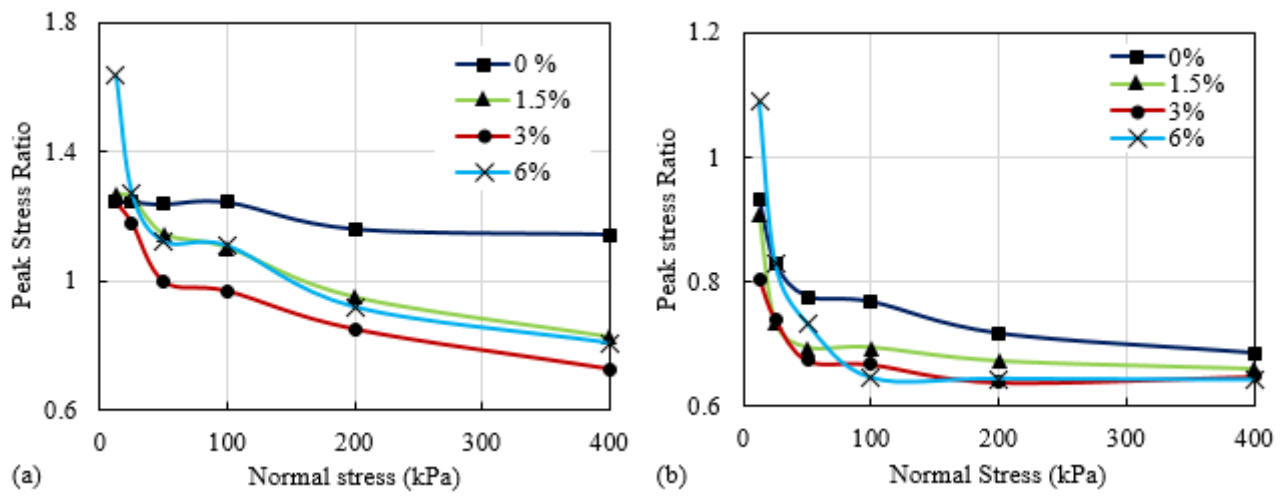


Figure 13

Effects of moisture content and normal stress on peak stress ratio: (a) compacted sand samples; (b) loose sand samples.

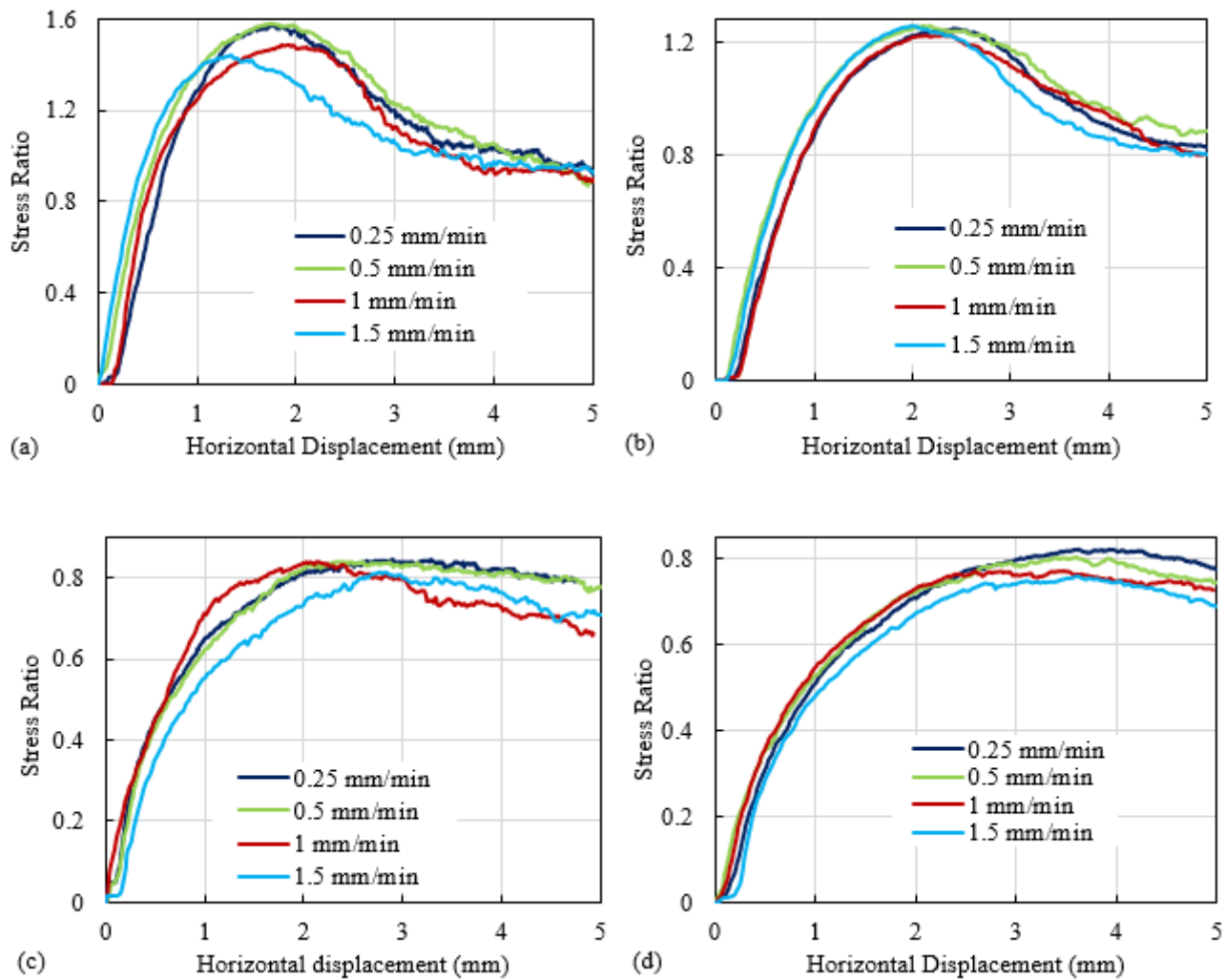


Figure 14

Effects of shear displacement rates (mm/min) on stress ratio: a) Dense sand: 100 kPa, b) Dense Sand: 400 kPa, c) Loose sand: 100 kPa, and d) Loose sand: 400 kPa

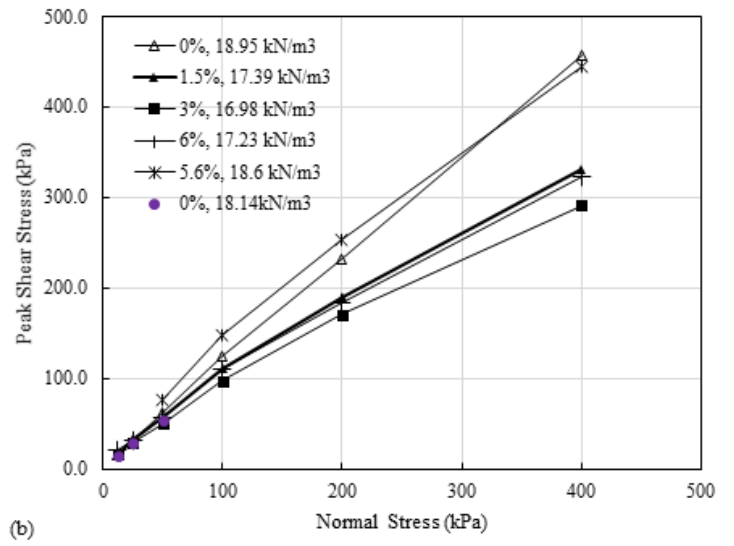
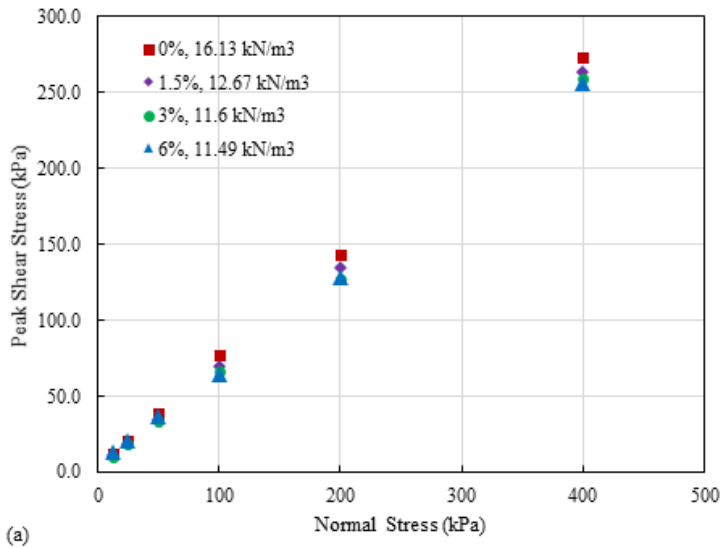


Figure 15

Shear stress versus normal stress plot for local sand: (a) Low dry unit weight and (b) High dry unit weight

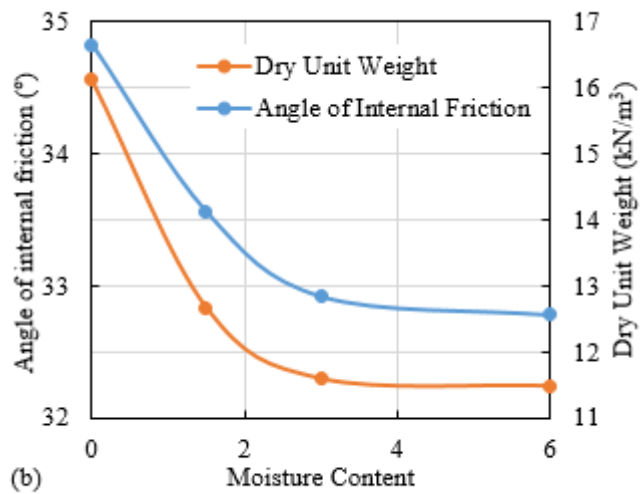
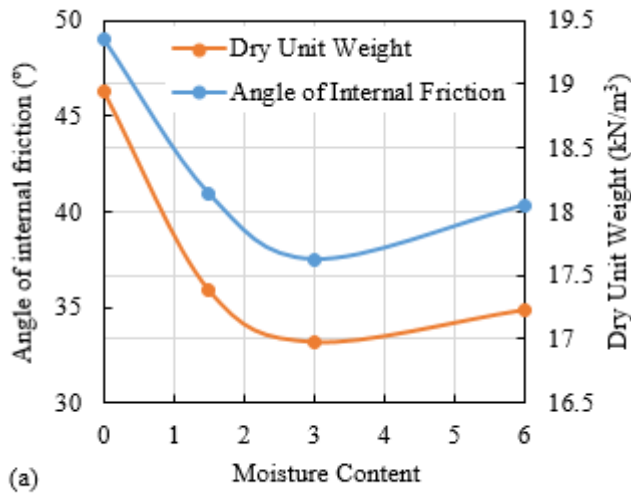


Figure 16

Effects of moisture content on the angle of internal friction and dry unit weight: (a) compacted sand and (b) uncompacted sand.

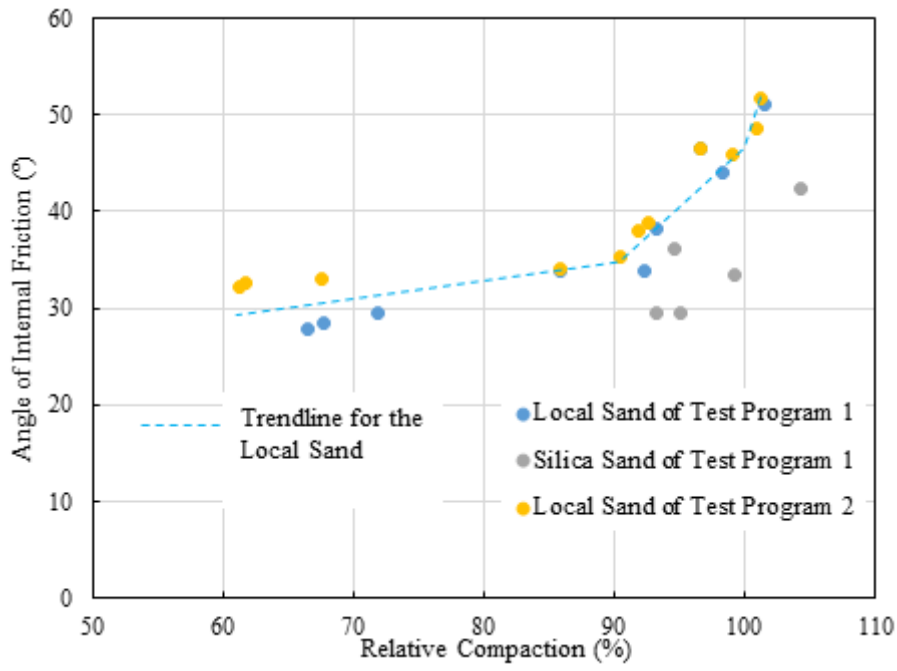


Figure 17

Variation of peak friction angle with relative compaction (Standard Proctor)